

# Modeling of Remote Field Eddy Current transient phenomena

M. Raugi

Dipartimento di Sistemi Elettrici ed Automazione, Università di Pisa,  
Via Diotisalvi 2, 56100 Pisa.

N. Ida

Department of Electrical Engineering, The University of Akron  
Akron, OH 44325, USA

**Abstract** - An integral formulation is presented and used for the analysis of the Remote Field Eddy Current (RFEC) transient phenomena. The model presented allows simple and accurate modeling of RFEC systems in the presence of axisymmetric defects.

The method has been validated first by comparison of the computed results with results obtained with an analytical model. Then the method was used to show that the Remote Field effect is mainly due to a direct induction effect rather than propagation effects.

The Remote Field effect phenomena are usually analysed using a steady state domain. However, the results obtained here have shown that detection of defects is not due to a steady state phenomenon, but depends mainly on the transient signal.

## 1. INTRODUCTION

The remote field effect is a Non Destructive Test method used for the testing of thick ferromagnetic materials for deep defects and in particular corrosion effects on the outer surface of tubes. This is particularly useful for gas lines but also for water lines and other thick walled tubes like oil well casings. The method relies on the use of very low intensity, low frequency electromagnetic fields which, unlike other types of tests are equally sensitive to defects on the outer surface of the tubes as on the inner surface. Thus, testing of thick materials can be easily performed from the accessible inner surface [1]. The RFEC testing probe is made of two coils separated at a distance of about two coil diameters and moving as a unit.

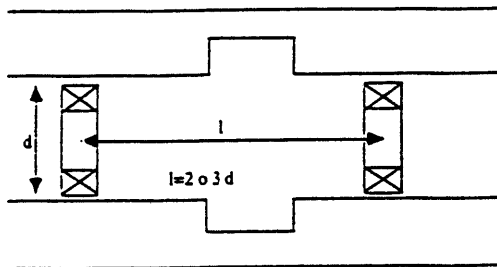


Fig. 1 RFEC probe configuration

One coil (the exciting coil) is driven with a sinusoidal current, and induces an output signal in the second coil (the pick-up coil). The probes move inside the tube at a constant velocity and the exciting current frequency is normally below 100 Hz. The theoretical basis of the remote field effect is not well established. In particular, some models [2-4] call for propagation effects to explain the equal sensitivity to

defects on either surface of the tubes. This model is not supported by experimental data or by the basic electromagnetic theory for low frequency fields. Existing models for the far field effect assume that all testing is done at such low speeds that the motion of the probe does not affect the signal obtained. This is far from being realistic. At low frequencies the speed effects on the signal are large and, in some cases, may even dominate. In this paper, we propose an integral model that incorporates speed effects, to correctly analyse the influence of speed on the calculated data.

## 2. MODEL

Due to the axial symmetry of the system, we divide the tube into elementary rings in which a uniform current is assumed.

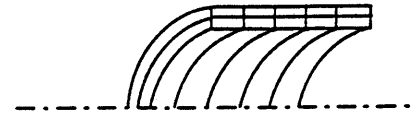


Fig 2 Subdivision of the tube into concentric rings

We write the Ohm's law at a point inside a generic ring as:

$$\frac{J}{\sigma} = -\nabla V - \frac{\partial A}{\partial t} \quad (1)$$

and then integrate both sides of this equation over the volume of the ring to obtain the integral equation [5]:

$$M_{je} \frac{\partial I_e}{\partial t} + v I_e \frac{\partial M_{pe}}{\partial x} + R_j I_j + \sum_{k=1}^{n-1} M_{jk} \frac{\partial I_k}{\partial t} + L_j \frac{\partial I_j}{\partial t} = 0 \quad (2)$$

This can be viewed as the electric equilibrium equation of the equivalent circuitual loop made of a resistance  $R$ , a self inductance  $L$  due to the ring itself and the mutual inductances  $M$  between the ring and all other rings that make up the tube and the coils. In Eq. (2) the subscript  $k$  identifies the rings 1 through  $n$ ,  $e$  identifies the exciting coil,  $I_k$  the current in the  $k$ -th loop of the network and  $I_e$  the current in the exciting coil.

To calculate the signal we consider only the  $n$  significant rings close to the coils. Writing this equation inside every ring, we obtain a system of  $n$  equations, that can be viewed as the equilibrium equations of the equivalent network shown in fig. 3. The equations thus obtained can be easily integrated using a classical Runge-Kutta method.

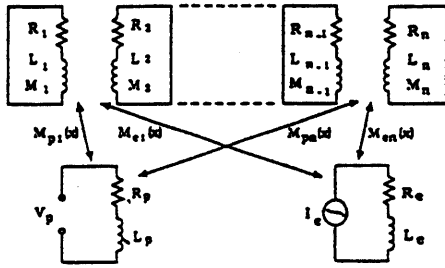


Fig. 3 Equivalent electric network

Axisymmetric defects in the tube are modeled by simply removing the rings corresponding to the volume of the defects. The corresponding loops in the equivalent network are also removed. The output signal  $V_p$  is:

$$V_p = \sum_{k=1}^n M_{pk} \frac{\partial I_k}{\partial t} + v I_k \frac{\partial M_{pk}}{\partial x} + M_{pe} \frac{\partial I_e}{\partial t} \quad (3)$$

The currents  $I_k$  are found from the solution of the system of equations for the equivalent network in fig. 3.

### 3. RESULTS

The model presented above has been tested by analyzing the geometry of TEAM Problem 9 [6], shown in fig. 4. The results for the tube without defects were compared with results obtained from an analytical solution.

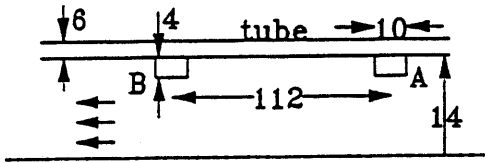


Fig. 4 Geometry of the Team problem 9

We first analyze the behaviour of results using a discretization of 150 x 3 rings, and varying the length of the tube.

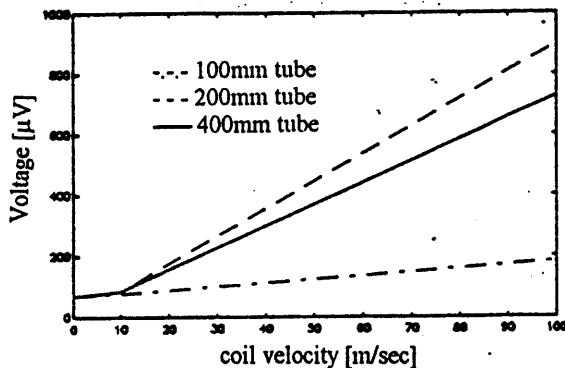


Fig. 5 Induced voltage vs. coil velocity, tube without defect

Fig. 5 shows the calculated and analytical voltage on the pick-up coil for different coil velocities and three different tube lengths. The results show that the length of the tube has

considerable influence on the correctness of the calculated data. To obtain good results, the distance between the exciting coil and the edge of the tube must be at least twice the distance between the exciting and pick-up coils. Next, we analyze the effect of discretization on the calculated data using a 400mm tube and three levels of discretization. Fig. 6 shows that the calculated results agree well with the analytical results even for a coarse discretization of 50 x 3 rings.

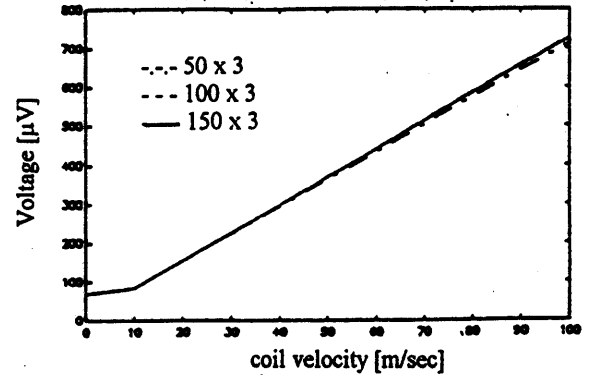


Fig. 6 Induced voltage vs. coil velocity, tube without defect

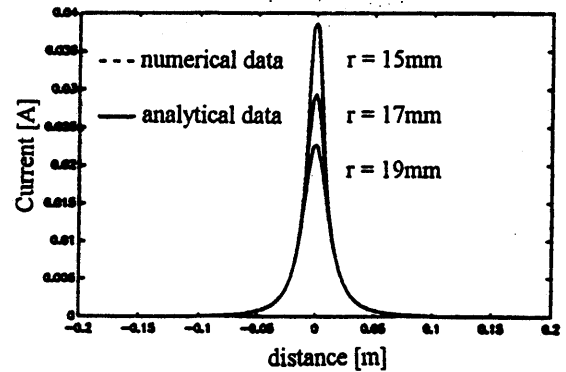


Fig. 7 Induced current modulus in the tube vs. distance from the exciting coil on three radii, for  $v = 0$ .

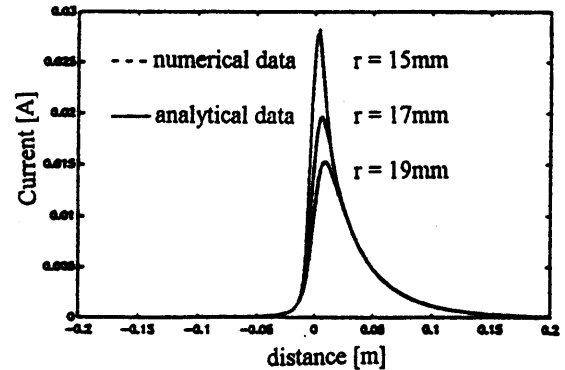


Fig. 8 Induced current modulus in the tube vs. distance from the exciting coil on three radii, for  $v = 100$  m/sec.

The effects of velocity are clearly shown by comparison of the analytically and numerically calculated induced currents in the tube. Fig. 7 and 8 show the induced currents at

three different radii in the tube for  $v=0$  and  $v=100$  m/sec for the previous geometry and discretization level.

Next, we study the geometry shown in fig. 9 considering a conductivity  $\sigma=2 \cdot 10^9$  (S/m) and a constant relative permeability  $\mu_r=1000$ , the exciting signal frequency is 50 Hz. For configurations which includes an axisymmetric defect, there is an analytical solution only for a non ferromagnetic tube [5], or for a ferromagnetic tube at zero coils velocity [7].

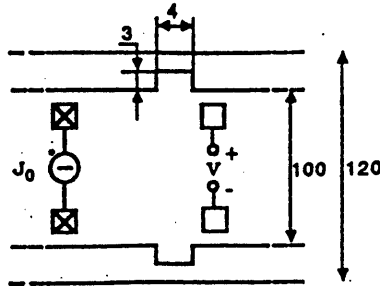


Fig. 9 RFEC geometry with an axisymmetric defects.

Fig. 10 and 11 show good agreement between the computed and analytical induced voltage and phase for a defect size of  $2 \times 4$  mm and different relative positions between the defect and the coils. In the following figures distance zero means that the pick up coil is exactly under the defect.

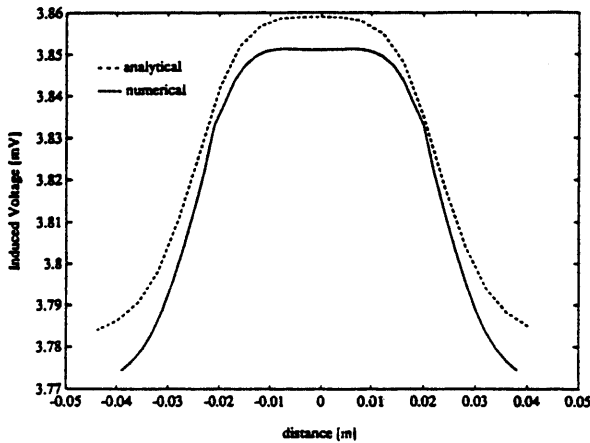


Fig. 10 Induced voltage vs coil position, tube with defect

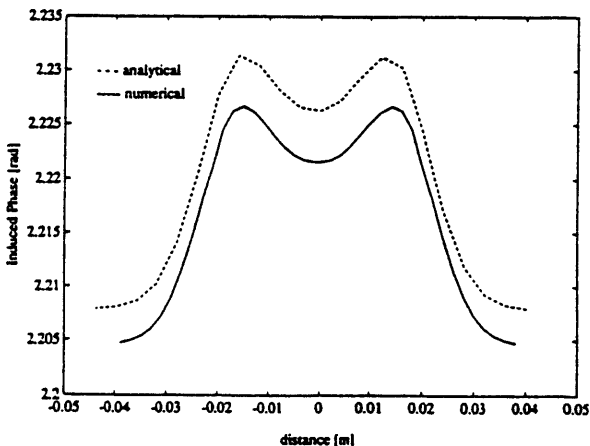


Fig. 11 Phase of the induced voltage vs. coil position, tube with defect

As a conclusion from the tests above, we observe that the characteristic "double bump" signal was only clearly detectable if the tube material has a high conductivity; copper for instance. The influence of tube length and discretization level on the results calculated for the cases shown in figures 7, 8, 10 and 11 is not shown here but these show the same trends as the results in fig. 4 and 5. The influence of the tube length is more pronounced than that due to discretization. This means that the proposed method does not require fine discretization for good results, even in presence of defects. One purpose of this method was to show that the RFEC is a direct induction effect. To do so we calculated the induced voltage for tubes with wall thickness of 7 cm. and 12 cm.

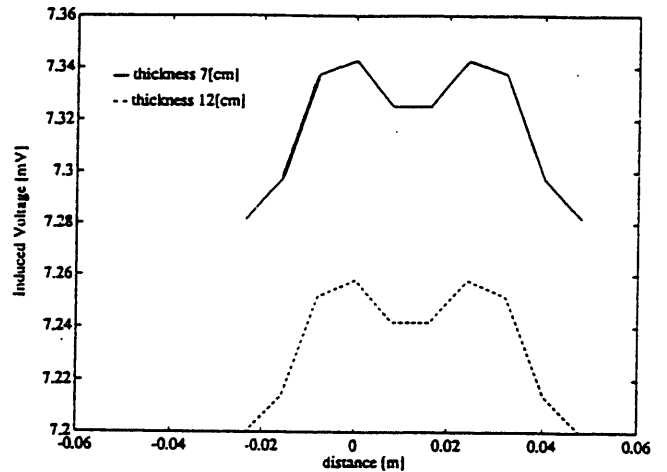


Fig. 12 Induced voltage vs coil position, thick tube with inner defect

Figure 12 shows that the induced voltage is still sensitive to the presence of an internal defect as the pick-up coil passes under the defect. In addition, the magnitude of the induced voltage is nearly equal for the two thicknesses tested, indicating that sensitivity is unrelated to wall thickness. Figures 13, and 14 show the transient induced voltage for different frequencies and probe velocity.

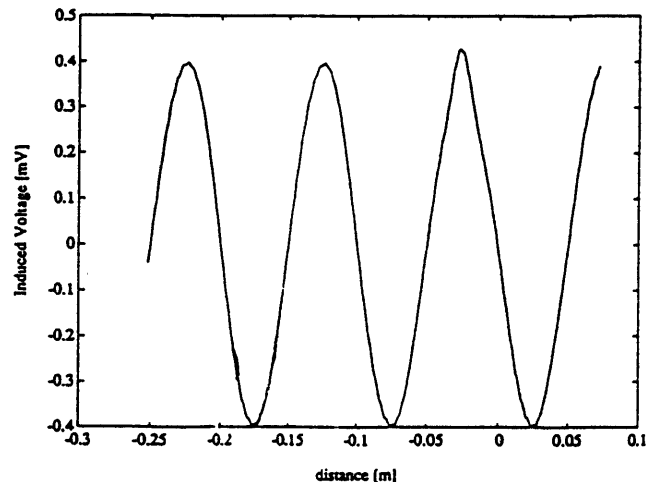


Fig. 13 Induced voltage vs. coil position,  $f=50$  Hz,  $v=5$ m/sec

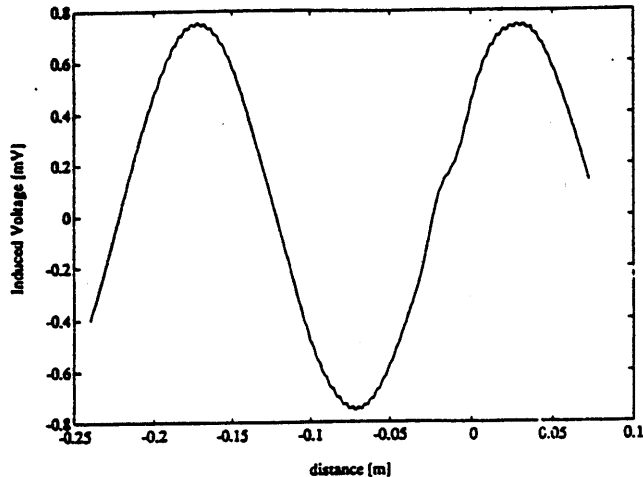


Fig. 14 Induced voltage vs. coil position,  $f=50$  Hz,  $v=10$ m/sec

The induced voltage has a typical transient behaviour, even for the lower velocities considered here. This behaviour cannot be related to steady state parameters. Furthermore, there is also a dependence between coil velocity and excitation frequency and detectability of the defect. In fact, at a frequency of 50 Hz, and a velocity of 10 m/sec, the pick-up signal is distorted, as shown in fig. 12, while at a velocity 5 m/sec the amplitude variation is clearer, and the defect can be discerned. Therefore, the conclusion is that there must be a high frequency/velocity ratio for clear defect detection. This is also pointed out in the figures 15 and 16.

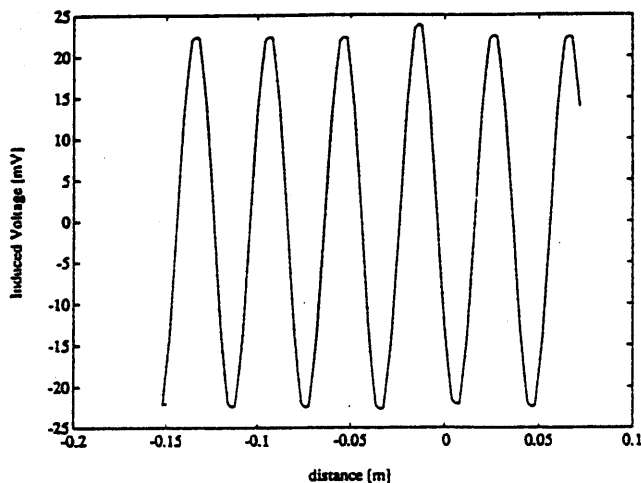


Fig. 15 Induced voltage vs. coil position,  $f=785$  Hz,  $v=5$ m/sec

Figure 15 shows a clearer variation of the pick-up signal in comparison with Fig. 12. This is accomplished by increasing the frequency from 50 Hz to 785 Hz. Fig. 16 shows that the sensitivity is unchanged if the frequency/velocity ratio is kept constant but with a frequency and velocity 10 times higher.

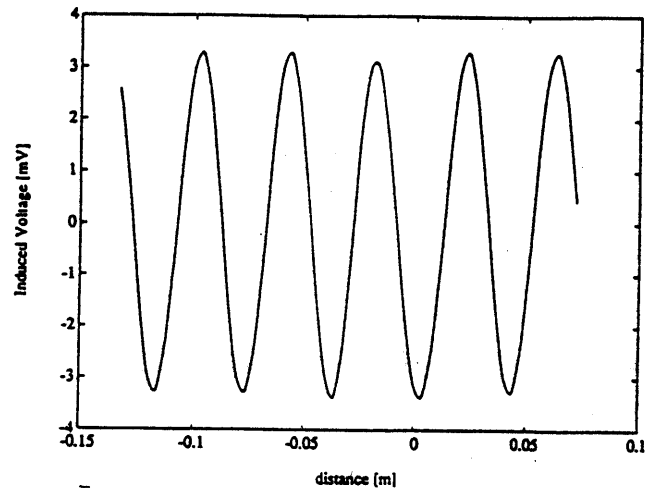


Fig. 16 Induced voltage vs. coil position,  $f=7850$  Hz,  $v=50$ m/sec

#### 4. CONCLUSIONS

The integral formulation presented here allows simple modeling of RFEC tests, including defects. Computation time is relatively short even in the presence of moving objects. The method has been validated first by comparison with analytical results. Application of the formulation for the analysis of the response of a RFEC testing apparatus has highlighted the importance of several aspects of the transient phenomena.

In particular, the output signal must be transient for complete understanding of defect detection process. Also, the importance of the relation between frequency of the exciting signal and coil velocity was pointed out.

#### REFERENCES

- [1] T.R.Schmidt, "The remote field eddy current inspection technique" *Materials Evaluations*, Vol. 42, no. 42, pp 225-230, 1984.
- [2] W. Lord, .S.Sun, S.S.Udpa, S.Nath, "A finite element study of the remote field eddy current phenomenon" *IEEE Trans on Mag.* Vo 24, p435, 1988
- [3] D.L.Atherton, B. Stamm, S. Sullivan, "The remote field through-wall electromagnetic inspection technique for pressure tubes" *Material Evaluation*, Vol. 44, p. 1544, 1986.
- [4] Y.S.Sun, " Finite element study of diffusion energ flow in low frequency eddy current field" *Materials Evaluations*, Vol. 47,pp 87, 1989.
- [5] N. Ida, M. Raugi, " Theoretical models for the Remote Field effect" *IEEE Trans. on Mag.* Vol 29, n. 2, March 1993.
- [6] "Problem 9 Velocity effects and low level fields in axisymmetric geometries" *Proc. of the European TEAM workshop and International Seminar on Electromagnetic field analysis*, Oxford, England, 23-25 April 1990, p323
- [7] N. Esposito, M. Raugi, A. Tellini: "A Quasi-Analytical Procedure for Magnetic Fields Analysis in Bounded Domains via Magnetization Currents" *IEEE Trans. on Mag.* Vol 31, n. 2, March 1995

